Proceedings of ASME FEDSM'03
4th ASME_JSME Joint Fluids Engineering Conference
Honolulu, Hawaii, USA, July 6-10, 2003

FEDSM2003-45512

# Vortex Induced Auto-Rotation of a Hinged Plate: A Computational Study

**Veeraraghavan Seshadri and Rajat Mittal**[1]

*Department of Mechanical and Aerospace Engineering*
*The George Washington University*
*Washington DC*

**H.S. Udaykumar**

*Department of Mechanical Engineering*
*University of Iowa*
*Iowa City, IA*

## ABSTRACT

Numerical simulations have been used to study the phenomenon of autorotation of a flat plate hinged about its center in a freestream. The focus of the paper is on examining the effect of Reynolds number and plate thickness ratio on vortex induced rotation. The numerical solver employed is based on a sharp interface, Cartesian grid method that allows us to simulate flow with moving boundaries on stationary Cartesian grids. Simulations indicate that vortex shedding is the primary instigator of the plate motion and the transition from fluttering to autorotation depends on both these parameters.

## 1. INTRODUCTION

Studies on fluid-structure interaction have to a large extent focused on translational and vibrational motions induced by the fluid flow. In contrast flow induced rotation has not been given significant attention. This is despite the fact that flow induced rotation finds application in areas as diverse as the functional morphology of plants and animals [2], meterology, aeroballistics [3], chemical processing and even fluidic micro assembly [4,16]. Another interesting fluid problem which has direct relevance to flow induced rotation, is the motion of a falling objects. Maxwell [1] published one of the first studies on the tumbling motion of a falling cards. In recent years the problem has been studied in detail by many researchers[3,5-7] but despite this it is fair to say that much more work is needed to understand further the details of the associated flow phenomenon. Here we have used a newly developed Cartesian grid method to study the flow-induced motion of a hinged plate which is pinned at its center and the details of this study are described in current paper.

## 2. FLOW CONFIGURATION AND SIMULATION APPROACH

The flow configuration used in all these simulations consist of a two dimensional flat plate with circular tip. The plate has a tip-to-tip length of $L$, thickness of $t$ and is pinned at its center. The plate is immersed in a free stream with a uniform velocity of $V_0$. The key governing non-dimensional parameters of the flow problem are the Reynolds number $\mathrm{Re} = LV_0/\nu$, plate thickness ratio $\tau = t/L$ and the non dimensional moment of inertia, $I^* = I/\rho_f L^4 w$. Here $L$, $w$, $t$ are the plate length, width and thickness respectively, $I$ the moment of inertia about its center and $\rho_f$ the fluid density. It is to be noted that these non-dimensional parameters would also govern the motion of a freely falling plate where $V_0$ would be the mean terminal velocity of the plate. Depending on the values of these parameters it is expected that the plate will either exhibits periodic oscillation (flutter) or end-to-end rotation (auto-rotation/ tumbling). The primary objective of the current study is to understand the role played by these parameters in determining the motion of the plate

The experimental study of Field et al. [6] on the motion of freely falling circular disks indicated that tumbling (end-over-end rotations) occurred for $I^* \geq 0.04$ and $\mathrm{Re} \geq 200$. Belmonte et al. [5] on the other hand, examined the motion of

[1] Corresponding Author
801 22nd St. NW, Suite T729
Washington DC 20052
mittal@seas.gwu.edu

rectangular flat plates and came up with a critical value of Froude number to be around 0.67. This Froude number is directly related to $I^*$ and gives a critical value of 0.037 for this parameter. Further experimental studies of Willmarth et al. [9] and Iverson [10] establishes critical $I^*$ values to be around 0.01 and 0.05 respectively above which autorotation was found to occur in both their experiments. It is therefore clear from the previous studies that the dependence of the plate motion transition with respect to $I^*$ is well established. In contrast, our understanding of the effect of $\tau$ and Re on this transition is somewhat more limited. For understanding better the effect of these two parameters on the induced motion, a series of simulations has been carried out by varying $\tau$ and Re. In all these simulations the value of $I^*$ was kept above 0.17 eliminated the dependence of flutter to rotation transition on this parameter.

**Numerical flow solver:** A previously developed Cartesian grid solver is employed in these simulations and details of the solution procedure can be found in [12] and [13]. The framework of the method developed in these papers is Eulerian-Lagrangian, i.e. the immersed boundaries are explicitly tracked as curves in Lagrangian fashion, while the flow computations are performed on a fixed Eulerian mesh. This affords the advantage of pure Lagrangian methods such as explicit interface information without ambiguities associated with *a-posteriori* reconstruction of the interface from an advected scalar (such as Volume-of-Fluid, Level Set or phase field). However, we dispense with mesh movement and thereby circumvent some of the problems associated with mesh management. In contrast with purely Eulerian interface capturing approaches (diffuse interface methods) the current method treats the immersed boundaries as sharp interfaces. The distinguishing feature of the present method is that the governing equations are discretized on a Cartesian grid which does not conform to the immersed boundaries. This greatly simplifies grid generation and also retains the relative simplicity of the governing equations in Cartesian coordinates.

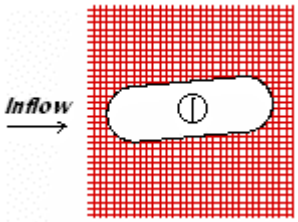


Figure1: Grid employed in the simulation. Every second grid point shown

Therefore, this method has distinct advantages over the conventional body-fitted approach in simulating flows with moving boundaries, complicated shapes or topological changes.

The interface is tracked using markers connected by piecewise quadratic curves parameterized with respect to the arc length. Details regarding interface representation, evaluation of derivatives along the interface to obtain normals, curvatures etc., have been presented in previous papers [12, 13] and are not repeated here. Also described in earlier papers are details regarding the interaction of the interfaces with the underlying fixed Cartesian mesh. These include obtaining locations where the interface cuts the mesh, identifying phases in which the cell centers lie, and procedures for obtaining a consistent mosaic of control volumes in the cells. This results in the formation of control-volumes which are trapezoidal in shape.

The solver employs a second-order accurate central difference scheme for the spatial discretization and a mixed explicit-implicit fractional step scheme for time advancement. An efficient multigrid algorithm is used for solving the pressure Poisson equation. The key advantage of this solver for the current flow is that the hinged plate is modeled on the stationary Cartesian mesh. Only those cells that are cut by the solid boundary are modified to account for the presence of solid boundary.

A large $62L \times 62L$ computational domain is employed for the current simulations. This significantly reduces the effect of boundaries interfering with the flow. A non uniform Cartesian mesh with 162×162 grid points is used which provides high resolution in the vicinity of the hinged plate as shown in the Fig 1. Freestream velocity conditions are imposed at the left, top and bottom boundaries and convective boundary condition is applied at the right boundary. In order to demonstrate the adequacy of the grid resolution and domain size simulations were carried out for a Reynolds number case of 600 on two different grids, one the 162×162 nominal grid and the other being a finer one with 50% more grid points in both the direction. Also domain adequacy has been verified by choosing again two different domains one being the nominal $62L \times 62L$ and the other being 50% more in length in both the direction. In all these test simulations key quantities such as mean and root-mean-square lift, drag and moment coefficients were computed. These values are found to vary by less than 3% from their nominal value thereby confirming the fidelity of the current simulations.

## 3. Simulation Results

Simulations of flow past the hinged plate have been carried out at Reynolds numbers of 50, 100, 200, 300,400 and 600 and thickness ratios of 1/2, 1/3 and 1/5. A summary of the results from these simulations is plotted plotted in Figure 2, which shows a parametric space of $\tau$, and Re. The range of values of $\tau$ and Re for which the plate executes angular oscillation (flutter) and rotational motion (autorotation) are indicated by open squares and filled squares respectively. The demarcation between the two regions of motion is a narrow region and is represented by the dotted curve as shown in the figure. In this region the plate was found to switch intermittently between both types of motion. The plot indicates that there is a minimum value of Reynolds number

below which auto rotation should never occur and this critical Reynolds number should occur some were between 100 and 200. This is in rough agreement with the conclusion of Fields et al. [6] for freely falling circular plates where it was found that a minimum Reynolds number value of about 200 was necessary for the tumbling to set in. It is also clear that as the thickness ratio increases, the transition to autorotation is found to occur

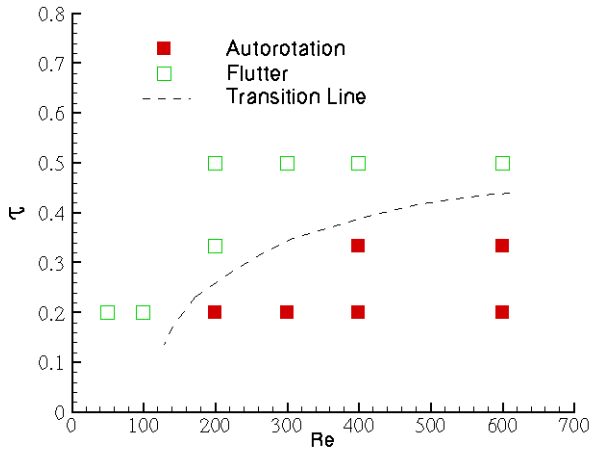


Figure 2. Phase plot showing region of transition from flutter to autorotation for the hinged plate

at increasingly higher values of Reynolds numbers. As expected the observed trend in the data suggests that as $\tau$ approaches 1 (i.e. the plate becomes a circular cylinder) the plate would not autorotate for any value of Reynolds number. To examine this behavior further let us consider three cases from our current study. First is the case for which Re = 200 and $\tau$ = 1 / 3 where autorotation is not observed. Figure 3a shows a span wise vorticity contour plot at one time instant for this case and this shows the presence of Karman vortex shedding in the wake of this plate. The second case chosen is this same plate at Re = 400 where autorotation is observed and Fig. 3b shows the vorticity contour plot for this case. The final case chosen is the Re = 400; $\tau$= 1/2 case which does not autorotate and its vorticity contours are shown in Fig. 3c. Comparing the first two cases we find even for plates of relatively low thickness ratios, the mere presence of vortex shedding does not necessarily lead to autorotation. On the other hand, comparison of the second and third case serves to show that even in the presence of relatively high Reynolds number vortex shedding, thick plates tend to resist autorotation. The question now is how to explain these observed trends in terms of the flow physics. It seems clear from our simulations that plate rotation is a result of the oscillatory moment produced on the plate due to vortex shedding. As the amplitude of this oscillatory moment increases, the plate tends to execute larger amplitude angular oscillations and for high enough moment amplitude, this leads to autorotation. The idea then is to explain why reduction in $\tau$ and increase in Re would tend to increase the moment amplitude. We put forth a simple explanation for this behavior. First, computations show that most of the moment is produced due to the surface pressure and not the shear stress. This is so because not only are shear stress levels relatively low at these Reynolds numbers, but the average moment arm for shear stress is smaller than that for pressure. Second, it appears that the pressure on the windward side of the plate does not contribute much in terms of moment and that the moment on the plate is produced primarily by low pressure on the leeward side of the plate due to the shedding of vortices. If we consider that the presence of a vortex near one of the tips of the plate in the lee side of the plate produces a uniform suction pressure on one half of the plate surface extending from the plate center to the tip of the plate where the vortex is located. For the plate with rounded tips, it can be shown that this uniform pressure distribution will produce a moment, which is proportional to (1-$\tau$). Thus, decreasing values of $\tau$ should increase the tendency of the plate to auto rotate. Now obviously, the pressure distribution due to vortex shedding is not uniform. In fact, as the Reynolds number increases, the vortices that roll up, tend to be of higher strength, are more compact and roll up closer to the tip of the plate. Thus, as the Reynolds number increases, the magnitude of the suction pressure increases, and furthermore, this higher suction pressure acts closer to the

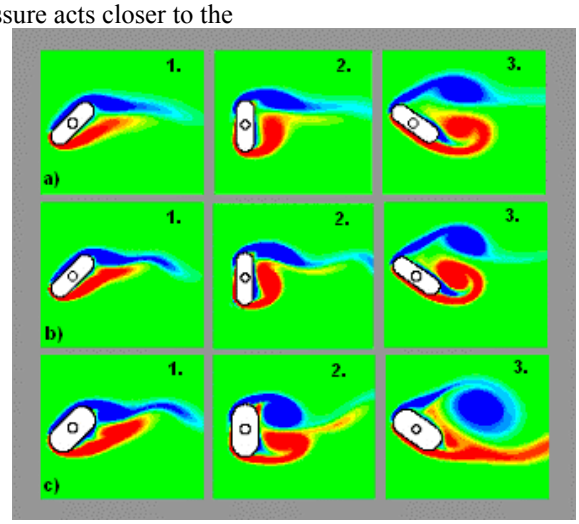


Figure3: Vortex contours at different stages of rotation for a) Re=200 (flutter), $t/L$=1/3 b) Re=400 (auto-rotating), $t/L$=1/3 and c) Re=400 (flutter), $t/L$=1/2

increases, the magnitude of the suction pressure increases, and furthermore, this higher suction pressure acts closer to the plate tip. This results in a higher moment and consequently, an increased tendency towards autorotation. In addition to the flutter-to-tumble transition, the current simulations also allow us to examine the scaling of the flutter/tumble frequency. Figure 4 shows the Strouhal frequency St = $\Omega L/V_0$ where $\Omega$ is

the flutter or tumble frequency obtained from examining the temporal variation of the plate angle plotted against the Reynolds number. Also plotted here is the variation of the vortex shedding Strouhal frequency for a 2D, normal fixed plate [14] and a circular cylinder [15]. It is evident from this plot that the flutter frequency is in reasonable agreement with the Strouhal frequency of these bluff bodies. This is expected since for low amplitude flutter, the vortex shedding from the hinged plate is expected to be quite similar to that observed for these bluff bodies. Interestingly, even the frequency for the autorotating cases is in reasonable agreement with the

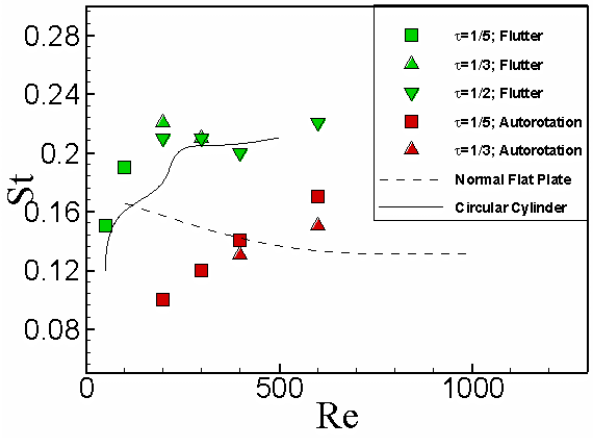


Figure 4. Variation of Strouhal number with Reynolds number for various cases

observed frequencies for the normal flat plate. This strongly suggests that the tumbling frequency is primarily determined by the Karman vortex shedding process. However, the vortex shedding process is itself altered by the autorotation (or tumbling) and that is most likely responsible for the variation in tumbling frequency with Reynolds number.

Figure 5 shows the values of drag and lift coefficients plotted against the thickness ratio. The filled triangle plotted on this figure represents the value of lift and drag coefficients obtained by Skews [11] at a Re~$10^5$. Note that in the work of Skews[11] plates with squared tips were used. Furthermore, the Reynolds number in that study was O($10^5$) which is significantly higher than the current study. Figure 5 however indicates a reasonable agreement between the experiments and the current simulations suggesting that once autorotation occurs, the hydrodynamic forces are relatively insensitive to the flow parameters.

In conclusion, the current simulations show that in the range of parameters studied here, the transition from flutter to tumble depends significantly on the thickness ratio and Reynolds number. The simulations suggest a simple physical explanation for this dependence and also allow us to hypothesize the effect that change in the cross sectional shape of the plate would have on this transition. Based on our results, we suggest that the flutter and tumble frequency of large aspect ratio plates is governed by the Karman vortex shedding process. Additional simulations are currently being carried out to understand other aspects of this flow configuration.

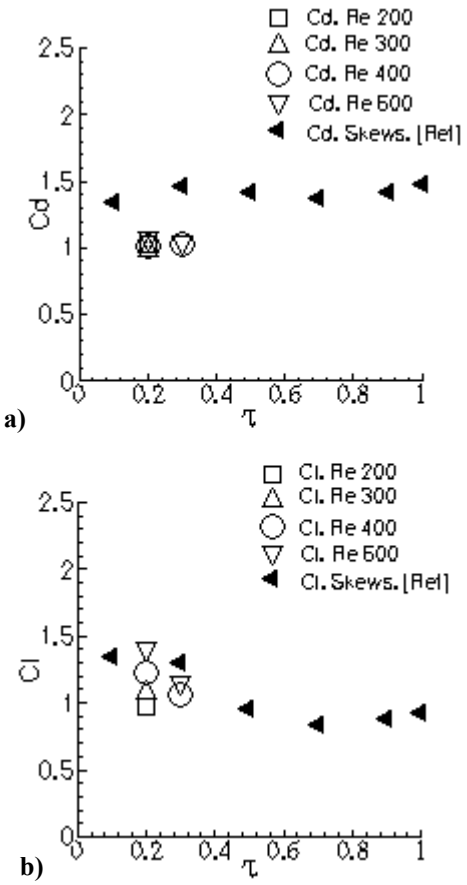


Figure 5. Drag and lift coefficients plotted against thickness ratio $\tau=t/L$ for the autorotating cases.

## REFERENCES


[1] Maxwell, J.C, 1853, "On a particular case of the descent of a heavy body in a resisting medium". Cambridge and Dublin Mathematical Journal **9**:115-118.

[2] A. Azuma, 1992, "The Biokinetics of Flying and Swimming," Springer-Verlag, Tokyo

[3] H. J. Lugt, 1983, "Autorotation," *Annual Review of Fluid Mechanics*.**15**, 123-147

[4] R. Mittal, V. Seshadri, S. E. Sarma and H. S. Udaykumar, 2002,"Computational Modeling of Fluidic Micro-Handling Processes," *Technical Proceedings of the 5th International Conference on Modeling and Simulation of Microsystems*, 388-391.

[5] A. Belmonte, H. Eisenberg and E. Moses, 1998,"From Flutter to Tumble: Inertial Drag and Froude Similarity in Falling Paper," *Physics Review Letters*, **81**, No 2, 345-348..

[6] S. B. Field, M. Klaus, M. G. Moore and F. Nori, 1997, "Chaotic dynamics of falling disks," *Nature*, **338**, 252-254.

[7] L. Mahadevan, W.S. Ryu, and A.D.T. Samuel 1999. "Tumbling Cards,". *Physics of Fluids* **11**(1),1-3.

[8] Y. Tanabe and K. Kaneko, 1998, "Behavior of a Falling Paper," *Physical Review Letters*, **73**(10), 1372-1375.

[9] W. W. Willmarth, N. E. Hawk and R. L. Harvey, 1964, "Steady and Unsteady Motions and Wakes of Freely Falling Disks," *Physics of Fluids*, **7**, No 2, 197-208 .

[10] J. D. Iverson, 1979, "Autorotating flat-plate wings:the effect of the moment of inertia, geometry and Reynolds number," *Journal of Fluid Mechanics*. **92**, Part 2, 327-348 .

[11] B. W. Skews., 1990,"Autorotation of rectangular plates," *Journal of Fluid Mechanics*, **217**, 33-40.

[12] T. Ye, R. Mittal, H. S. Udaykumar and W. Shyy, 1999, "An Accurate Cartesian Grid Method for Viscous Incompressible Flows with Complex Immersed Boundaries," *Journal of Computational Physics*, **156**, 209-240.

[13] H. S. Udaykumar R. Mittal, P. Rampunggoon and A. Khanna, *J. Comp. Phys*. 174, 245-380 (2001).

[14] F. M. Najjar and S. P. Vanka, *Int. J. Numer. Meth. Fluids*

21, 525-547 (1995).

[15] C. H. K. W. Williamson, *Ann. Rev. Fluid Mech*. 28, 477 (1996).

[16] H.-J. J. Yeh and J.S. Smith, 1994,"Fluidic Assembly for the Integration of GAAs Light-Emitting Diodes on Si Substrates". *IEEE Photonics Technology Leters*, **6**, 706-708.